

1 Evidence of Chlordecone Resurrection by Glyphosate in French 2 West Indies

3 Pierre Sabatier,* Charles Mottes, Nathalie Cottin, Olivier Evrard, Irina Comte, Christine Piot,
4 Bastien Gay, Fabien Arnaud, Irène Lefevre, Anne-Lise Develle, Landry Deffontaines, Joanne Plet,
5 Magalie Lesueur-Jannoyer, and Jérôme Poulenard



Cite This: <https://dx.doi.org/10.1021/acs.est.0c05207>



Read Online

ACCESS |



Metrics & More

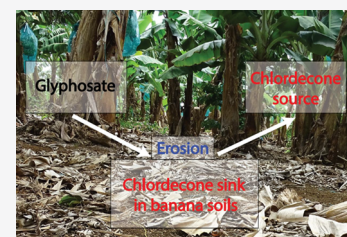


Article Recommendations



Supporting Information

6 **ABSTRACT:** The widespread use of pesticides in agriculture during the last several decades has
7 contaminated soils and different Critical Zone (CZ) compartments, defined as the area extended
8 from the top of the vegetation canopy to the groundwater table, and it integrates interactions of
9 the atmosphere, lithosphere, biosphere, and hydrosphere. However, the long-term fate, storage,
10 and transfer dynamics of persistent pesticides in CZ in a changing world remain poorly
11 understood. In the French West Indies, chlordecone (CLD), a toxic organochlorine insecticide,
12 was extensively applied to banana fields to control banana weevil from 1972 to 1993 after which
13 it was banned. Here, to understand CZ trajectories we apply a retrospective observation based
14 on marine sediment core analysis to monitor long-term CLD transfer, fate, and consequences in
15 Guadeloupe and Martinique islands. Both CLD profiles show synchronous chronologies. We hypothesized that the use of
16 glyphosate, a postemergence herbicide, from the late 1990s onward induced CZ modification with an increase in soil erosion and led
17 to the release of the stable CLD stored in the soils of polluted fields. CLD fluxes drastically increased when glyphosate use began,
18 leading to widespread ecosystem contamination. As glyphosate is used globally, ecotoxicological risk management strategies should
19 consider how its application affects persistent pesticide storage in soils, transfer dynamics, and widespread contamination.



20 ■ INTRODUCTION

21 The Critical Zone (CZ) may be defined as the reactive skin of
22 our planet within which most of its coupled physical, chemical,
23 biological, and geological processes operate together to
24 support life.¹ The emergence of human societies as a geological
25 factor modified these subtle equilibria under natural forces
26 (climate and tectonic),² resulting in unprecedented biodiversity
27 loss, biogeochemical disruptions, and modifications of the
28 erosion cycle³ leading to potential threats to the future of
29 humanity.⁴ In recent decades, the sediment fluxes in CZ
30 associated with the erosion of cultivated soils have greatly
31 increased in response to changes in agricultural practices⁵ such
32 as deforestation, overgrazing, tillage, and unsuitable agricultural
33 practices with the use of herbicides.⁶ Over the last several
34 decades (last 70 years), the use of many chemical substances to
35 control disease (fungicides), insect damage (insecticides), and
36 weed competition (herbicides) in cropland dramatically rose.⁷
37 Organochlorine insecticides such as dichlorodiphenyltrichloro-
38 ethane (DDT, C₁₄H₉Cl₅) or chlordecone (CLD, C₁₀Cl₁₀O)
39 are classified as persistent organic pollutants by the Stockholm
40 convention (<http://www.pops.int/>) but have been extensively
41 used worldwide. Their use has been progressively prohibited
42 since the 1970s because of their biomagnification, high toxicity,
43 and long-term persistence in the environment. A well-known
44 example is the contamination from the Hopewell CLD
45 production plant in the United States between 1965 and
46 1975 that resulted in high worker exposure and massive

pollution of over 160 km of the James River,⁸ which lasted for
several decades.⁹ Despite CLD being extensively used
worldwide, very few studies have documented its adverse
effects on the environment excepted in the Caribbean area. In
the French West Indies (FWI, Figure 1a) CLD was used to
control banana weevil during two periods: (1) 1972–1978
under the trade name Kepone, manufactured at Hopewell and
(2) 1982–1993 under the trade name Curlone. CLD was
banned worldwide in 1992 except in the FWI where it was
authorized until 1993 by the French government. However,
CLD is still persistent in most of the CZ compartments such as
soils,¹⁰ crops,¹¹ freshwater,¹² and coastal¹³ ecosystems until
pelagic cetaceans,¹⁴ with potential for severe toxic effects to
human populations¹⁵ with one of the highest prostate cancer
incidence in the world because of CLD exposure¹⁶ and the
related highest mortality rates.¹⁷ These studies suggest that a
significant amount of CLD is being transferred to the ocean,
raising the question of contamination provenance and its long-
term environmental fate for ecotoxicological management
strategies.

Received: August 3, 2020

Revised: January 6, 2021

Accepted: January 14, 2021

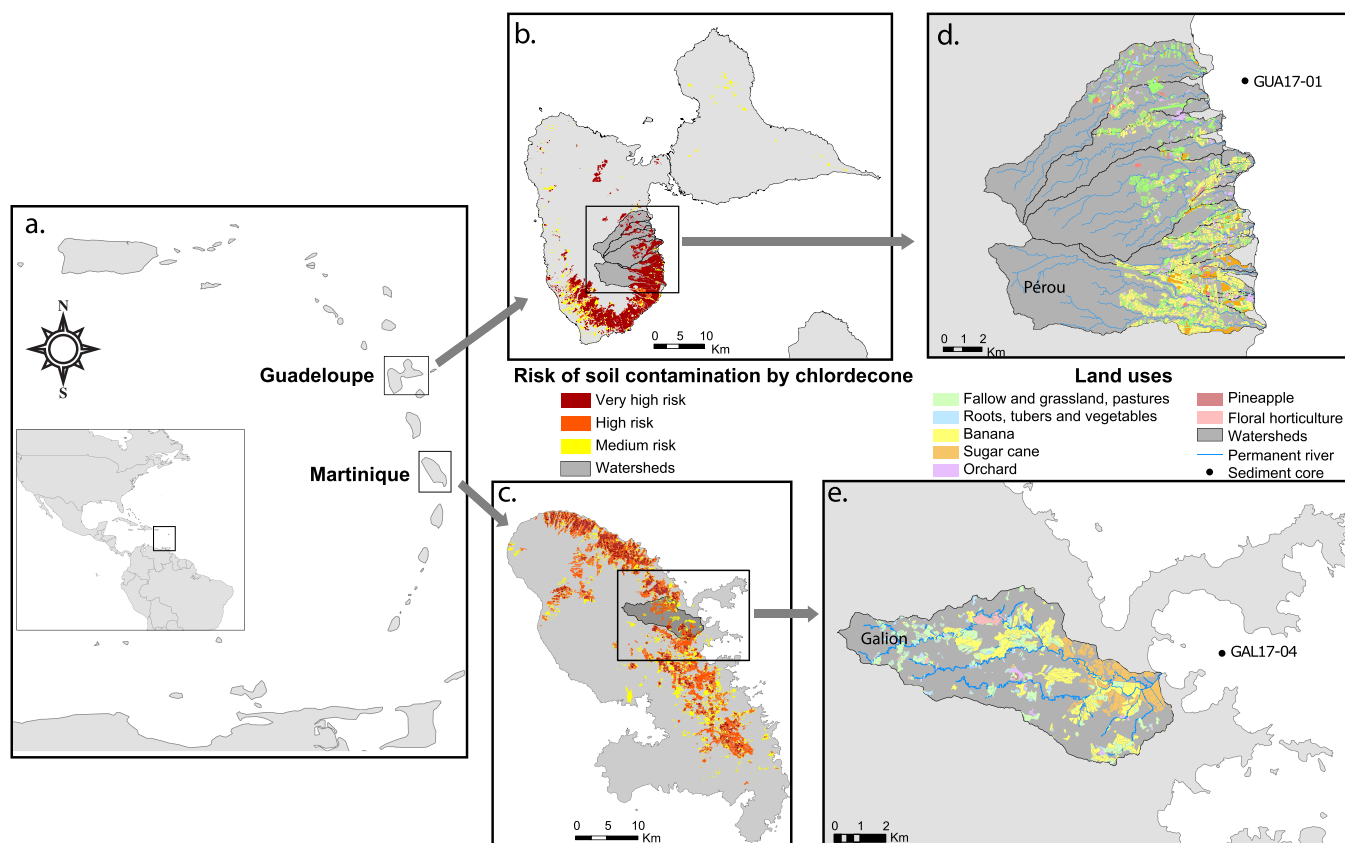


Figure 1. (a) Map of the Caribbean island arc with the localization of two French islands (Guadeloupe and Martinique). (b, c) Maps of Guadeloupe and Martinique showing the risk of soil contamination by CLD (very high, high, and medium risk); the dark gray area indicates the study area. (d, e) Localization of the studied watershed (dark gray) according to land use. Different colors indicate the types of crops, and banana plantations are indicated in yellow. Two sampled marine sediment cores GUA17-01 and GAL17-04 are indicated by black dots. Note that the sediment core from Guadeloupe (d) was not collected off the estuary of the monitored Pérou River because of the absence of fine sediment in the coastal zone at this location. Pérou (Guadeloupe) and Galion (Martinique) river watersheds (d, e) were also sampled for detailed information, see Figure S1. Land use data of 2017 were made available by the French Directions of Agriculture and Forestry of Martinique and Guadeloupe (DAAF Martinique and Guadeloupe). Risk of soil contamination by CLD was made available by Préfecture of Martinique and Préfecture of Guadeloupe, for their design see refs.^{19,32–34}

67 In the FWI, interactions between agricultural practices such
 68 as CLD application (~ 3 kg/ha/yr), tillage, plant cover,
 69 irrigation, and pedoclimatic conditions lead to high variability
 70 in the contamination level of soils^{18,19} (Figure 1b,c). CLD
 71 persistence in soils is explained by its (1) hydrophobicity,
 72 resulting in a high affinity for soil organic matter (high Koc 2.5
 73 to 20 $\text{m}^3 \cdot \text{kg}^{-1}$);¹⁰ (2) physical sequestration in the fractal
 74 structure of soils containing allophanic clay, such as
 75 Andosols,²⁰ which are typical of the volcanic FWI; and (3)
 76 poor biodegradability under aerobic conditions because of its
 77 chemical structure.²¹ Depending on the soil type and
 78 considering negligible CLD degradation, it was estimated
 79 that CLD could remain in soil for at least several decades and
 80 up to centuries.¹⁰ Thus, surface soil horizons act as reservoirs
 81 of CLD, gradually releasing this chemical into ground-
 82 water^{19,22,23} or bound to soil particles eroded by surface
 83 runoff.²⁴ Thus, if erosion of cultivated soils increases in
 84 response to changes in agricultural practices, soils will be
 85 converting from sinks to sources of pesticides. It has been
 86 demonstrated, through monitoring plots, simulation experi-
 87 ments, and retrospective observation that the massive use of
 88 postemergence herbicides such as glyphosate since the late
 89 1990s has had a strong effect on soil erosion, as it acts on grass
 90 development and leads to permanently bare soil, as has been

shown in vineyards^{6,25} clementine,²⁶ and rubber plantations.²⁷
 91 The present study was designed in order to test the hypothesis
 92 of enhanced CLD remobilization because of glyphosate
 93 application through the erosion of contaminated soils, as
 94 previously observed in vineyards with DDT remobilization.⁶
 95 To test this hypothesis, in the context of intensive
 96 glyphosate application,²⁸ we applied a retrospective observa-
 97 tion^{6,29,30} based on the analysis of marine sediment cores
 98 in order to monitor long-term CLD transfer from watersheds.
 99 Indeed, CZ is subjected to processes that occur at various time
 100 scales which implies that its trajectories must be documented
 101 over longer time periods much longer than direct observation
 102 experiments.³¹ A retrospective observation hence allows us to
 103 extend into the past monitoring observations thanks to dated
 104 sediment cores and associated proxies. In the present study,
 105 downcore contaminant profiles were associated with high-
 106 resolution sedimentological and geochemical proxies. Short-
 107 lived radionuclides provide a precise core chronology and the
 108 evolution of erosion patterns.⁶ The two investigated water-
 109 sheds were the Pérou River²³ in Guadeloupe and the Galion
 110 River¹⁹ in Martinique (Figure 1d,e). These watersheds present
 111 high to very high CLD soil risk contamination (Figure 1b,c).
 112 Both watersheds are mainly occupied by banana and sugar
 113 cane plantations (Figure 1d,e). Large cropped areas in the
 114

115 Galion watershed belong to large farms, while Pérou farmers
116 are mostly smallholders.

117 ■ MATERIALS AND METHODS

118 **Sampling.** A 1.13 m long core registered as GAL17–04
119 (N° IGSN TOAE0000000573) was collected in the Baie du
120 Galion in Martinique (WGS84: 14.72801600; –60.91658800)
121 at 15 m below sea level on April 2017. A 1.33 m long core
122 registered as GUA17–01 (N° IGSN TOAE0000000567) was
123 collected in Petit Cul-de-Sac Marin in Guadeloupe
124 (16.16857500; –61.56900800) at 13.3 m below sea level on
125 April 2017. Both cores were sampled using an Uwitec gravity
126 corer with a hammer from a small boat. Surface soil horizons
127 were sampled on the Galion (Martinique, $n = 44$) and Pérou
128 (Guadeloupe, $n = 35$) watersheds under different soil types
129 (Nitisol, Andosol, and Ferralsols) and land use contexts
130 (different crop types, forest, river sediment, and channel bank),
131 as illustrated in Figure S1. At the Grand Galion gauging
132 station, two floods were sampled on 19 December 2013 and on
133 23 December 2013. During both floods, 24 water samples (330
134 mL each) were taken every 6 min with an automatic sampler
135 (Sigma SD900) when the limnimetric level of the river
136 exceeded 80 cm (i.e., $1.85 \text{ m}^3 \cdot \text{s}^{-1}$). Using this protocol, each
137 flood was sampled for 2 h 24 min, with a 6 min resolution.
138 Water discharges during the two floods were also measured
139 with a pressure sensor. The discharges of both floods were
140 provided by DEAL (The French Environment, Planning and
141 Housing Department). By the end of each flood, 24 flasks had
142 been collected. For both floods, because of material availability
143 and logistical constraints, we selected 18 flasks for particle
144 filtration. The selection retained the maximum variations in
145 water color among the flasks and thereby the maximum
146 variability in the particle content among the samples. Using a
147 vacuum pump and $0.7 \mu\text{m}$ fiberglass filters (Whatman cat no
148 1825–047), we separated the dissolved fraction ($< 0.7 \mu\text{m}$)
149 from the particulate fraction ($> 0.7 \mu\text{m}$) for each of the 18
150 flasks collected during each flood. The particulate and
151 dissolved fractions were analyzed for CLD at the Laboratoire
152 Départemental d'Analyses de la Drôme (LDA26), which is
153 COFRAC (French Accreditation Committee) accredited. The
154 results are presented with a $\pm 30\%$ error interval, and the
155 limit of quantification (LOQ) was $0.01 \mu\text{g} \cdot \text{L}^{-1}$ for the
156 dissolved fraction and $10 \text{ ng} \cdot \text{g}^{-1}$ for the particulate fraction.
157 According to the analytical requirements of the laboratory for
158 CLD analysis, samples were pooled (Table S1) to obtain the
159 minimum (0.5 g) amount of solid, but the samples were kept
160 separate according to the flood rise, flood peak, and flood fall.

161 The mass of sediment in each composite sample varied
162 between 0.510 and 0.891 g, while the volume of water filtered
163 from the composite samples varied between 200 and 950 mL.
164 **Logging.** In the laboratory, the cores were split lengthwise,
165 photographed, and logged in detail, noting all physical
166 sedimentary structures. The grain size distributions of both
167 cores were determined using a Malvern Mastersizer 2000
168 (Isterre) with a continuous interval of 2 cm and ultrasound
169 during measurements. Cores were also cut at 2 cm depth
170 intervals, and a specific volume was dried at $60 \text{ }^\circ\text{C}$ for 4 days to
171 determine the dry bulk density (DBD); then, the loss of
172 ignition (LOI) of each interval was measured using the
173 protocol of Heiri.³⁵ The LOIs at 550 and $950 \text{ }^\circ\text{C}$ correspond
174 to the percent of organic and carbonate contents of the
175 sediment, respectively. The noncarbonate igneous residue
176 (NCIR, express in %) of each sample was obtained by

removing the LOI550 and LOI950 from the initial dry weight. 177
The terrigenous mass accumulation was calculated as $\text{NCIR} \times 178$
 $\text{DBD} \times \text{sedimentation rate}$, expressed in $\text{g} \cdot \text{cm}^{-2} \cdot \text{yr}^{-1}$. X-ray 179
fluorescence (XRF) analysis was performed on the surfaces of 180
the split sediment cores, which had been covered with $4 \mu\text{m}$ 181
thick Ultralene, at 2 mm intervals using an Avaatech core 182
scanner (EDYTEM). The geochemical data were obtained 183
with various tube settings: 10 kV at 0.15 mA for 15 s for Al, Si, 184
S, K, Ca, Ti, and Fe and 30 kV at 0.2 mA for 20 s for Cu, Zn, 185
Br, and Sr.³⁶ Three replicates were measured every 10 cm to 186
estimate the standard deviation. Each individual power 187
spectrum was deconvoluted into relative components (in- 188
tensities), expressed in counts per second. The principal 189
component analysis (PCA) was performed using R software. 190

Radionuclide Measurements. Surface soil horizons were 191
sampled in the Galion ($n = 44$) and Pérou ($n = 35$) watersheds 192
at locations with different soil types and land use contexts, as 193
illustrated in Figure S1, to assess whether erosion is an 194
important mechanism on plantations through short-lived 195
radionuclide analyses. The two marine sediment cores 196
collected in Petit Cul-de-Sac Marin (GUA17–01, Guade- 197
loupe) and Galion Bay (GAL17–04, Martinique) were 198
analyses for short-lived radionuclides to establish sediment 199
chronology (Tables S2 and S3). Prior to analyses, samples 200
from the watershed soils and core sediment were dried at 40 201
 $^\circ\text{C}$ for ~ 48 h, the watershed samples were sieved to 2 mm, and 202
all samples were ground to a fine powder in an agate mortar 203
and pressed into 15 or 60 mL polyethylene containers 204
depending on the quantity of material available for analysis. 205
Radionuclide activities were determined by gamma spectrom- 206
etry using coaxial N- and P-type HPGe detectors (Canberra/ 207
Ortec) at the Laboratoire des Sciences du Climat et de 208
l'Environnement (Gif-sur-Yvette, France). The ^{137}Cs activity 209
(half-life: 30.17 y) was measured from the 661.7 keV emission 210
peak. The $^{210}\text{Pb}_{\text{xs}}$ activity (half-life: 22.3 y) was calculated by 211
subtracting the supported activity (determined by using two 212
 ^{226}Ra daughters), the ^{214}Pb activity (average count number at 213
295.2 and 351.9 keV), and the ^{214}Bi activity (609.3 keV) from 214
the total ^{210}Pb activity measured at 46.5 keV.³⁷ Counting 215
efficiencies and calibration were determined using certified 216
International Atomic Energy Agency (IAEA) standards (IAEA- 217
444, 135, 375, RGU-1, and RGTh-1) prepared in the same 218
containers as the samples. 219

Pesticide Analysis. Pesticide analyses were performed on 220
samples from cores GUA17–01 ($n = 30$) and GAL17–04 ($n =$ 221
28) using an ALTHUS 30 ultraperformance liquid chromatog- 222
raphy system (PerkinElmer, USA) coupled in tandem to a 223
triple quadrupole mass spectrometer equipped with an 224
electrospray ionization source (PerkinElmer Q-Sigth 200). 225
For CLD and chlordecol (CLO), 3 g of lyophilized dry 226
sediment was extracted using an accelerated solvent extraction 227
system (ASE200, Dionex). The organic extract was then 228
evaporated, purified, and passed through a $0.2 \mu\text{m}$ filter before 229
analysis. The limit of detection (LOD, corresponding to a 230
signal-to-noise ratio of 3) and LOQ (corresponding to a signal- 231
to-noise ratio of 10) were 0.22 and $0.67 \text{ ng} \cdot \text{mL}^{-1}$ for CLD and 232
 0.1 and $0.3 \text{ ng} \cdot \text{mL}^{-1}$ for CLO, respectively. For glyphosate and 233
aminomethylphosphonic acid (AMPA), 1 g of lyophilized dry 234
sediment was added to 10 mL of 0.5 M KOH and vortexed for 235
1 min. Glyphosate-2- ^{13}C 15N and AMPA- ^{13}C 15N standard 236
solutions were added as internal standards to a final 237
concentration of $100 \text{ ng} \cdot \text{mL}^{-1}$ each. The extract was 238
centrifuged, and the water extract was filtered through a 0.2 239

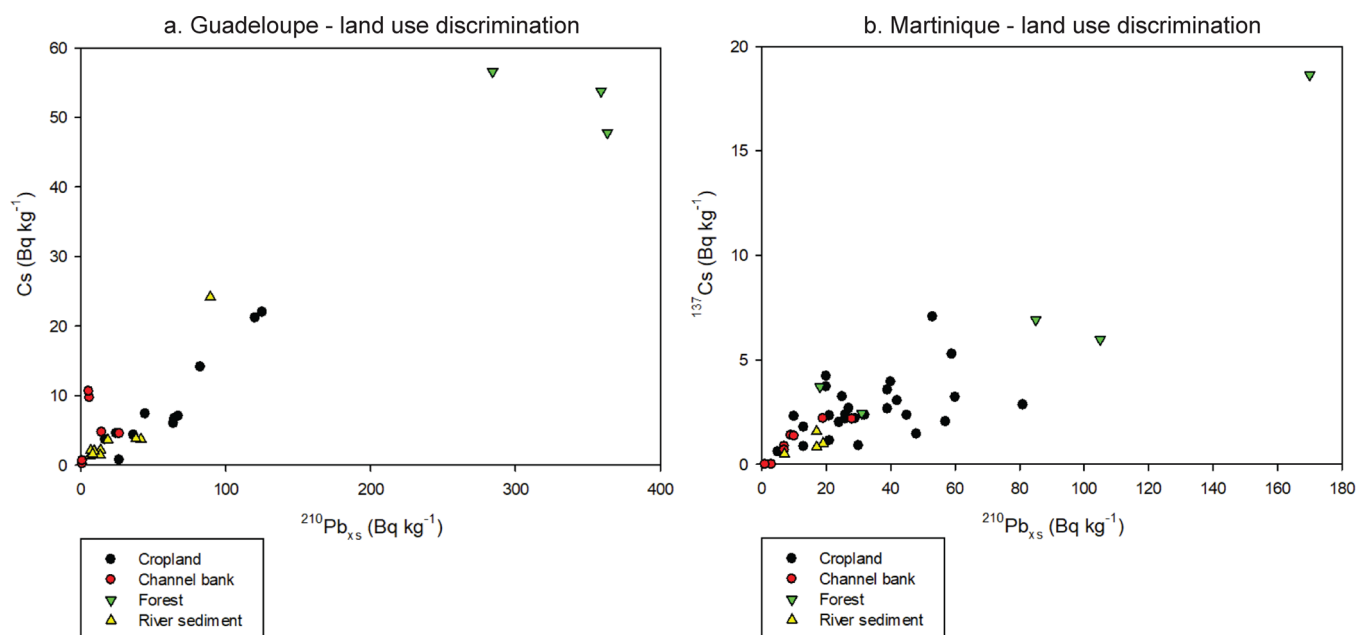


Figure 2. (a, b) $^{210}\text{Pb}_{\text{xs}}$ versus ^{137}Cs activities in the Pérou (Guadeloupe) and Galion (Martinique) river watersheds. Data are presented for the different land use conditions: cropland, forest, river sediment, and channel bank. Forest samples are enriched in ^{137}Cs and $^{210}\text{Pb}_{\text{xs}}$, while channel banks are depleted in both radioisotopes.

240 μm nylon filter and analyzed immediately after preparation.
 241 The LOD and LOQ were 2 and 6 $\text{ng}\cdot\text{mL}^{-1}$ for glyphosate and
 242 1 and 3 $\text{ng}\cdot\text{mL}^{-1}$ for AMPA, respectively. Detailed protocols
 243 are presented in the [Supporting Information](#). Pesticide fluxes
 244 were calculated as $\text{DBD} \times \text{sedimentation rate} \times [\text{pesticide}]$
 245 and expressed in $\text{mol}\cdot\text{g}\cdot\text{cm}^{-2}\cdot\text{y}^{-1}$.

246 ■ RESULTS AND DISCUSSION

247 **On Land Erosion.** Samples under forest cover, found in
 248 upper catchment areas exposed to the highest precipitation
 249 levels, were systematically enriched in ^{137}Cs and $^{210}\text{Pb}_{\text{xs}}$ relative
 250 to channel bank samples ([Figure 2](#)). The fallout radionuclide
 251 activities detected in cropland samples collected on banana and
 252 sugarcane plantations showed intermediate levels between
 253 those detected in forests and channel banks ([Figure 2](#)). The
 254 results show that the sediment originates from a mix of
 255 cropland (exposed to rainfall enriched in fallout radionuclides)
 256 and channel bank soils (sheltered from rainfall and fallout and
 257 depleted in radionuclides as demonstrated by Evrard et al.³⁸
 258 These samples show that the banana and sugarcane plantations
 259 provide a significant supply of sediment to river systems on
 260 these islands through erosional processes.

261 **Sediment Core and CLD Chronology.** The two marine
 262 sediment cores collected in Petit Cul-de-Sac Marin (GUA17–
 263 01, Guadeloupe) and Galion Bay (GAL17–04, Martinique)
 264 ([Figure 1d,e](#)) were characterized in terms of their particle size,
 265 LOI, XRF mineral geochemistry, and pesticide contents. Both
 266 cores contained relatively homogeneous olive-brown silt
 267 sediment. No noticeable variations in either the organic
 268 content or grain size distribution were observed ([Figure S2](#)).
 269 These parameter variations hence could not have affected the
 270 absorption/degradation of pesticides within the accumulated
 271 sediment.⁶ PCA on XRF data ([Figure S3](#)) showed two
 272 sediment end-member³⁹ inputs from the watershed, with
 273 organic matter and metallic pollutant contents and the marine
 274 carbonate productivity. The geochemical data were in good
 275 agreement with the LOI indicating an upward increase in

terrestrial inputs from the watershed (reflected by the Fe 276
 content) while carbonate productivity (reflected by the Ca 277
 content) decreased ([Figure S3](#)). Accordingly, the Fe/Ca ratio 278
 was used as a high-resolution proxy for the terrigenous 279
 fraction. 280

A chronological framework was established with the *serac* R 281
 package⁴⁰ from measurements of short-lived radionuclides, 282
 constrained by the identification of historical hurricane event 283
 deposits ([Figure 3](#), [Tables S2 and S3](#)) as ^{137}Cs did not provide 284
 an interpretable profile in relation to its desorption/migration 285
 in marine sediments.⁴¹ The Fe/Ca data in the GUA17–01 and 286
 GAL17–04 cores led to the identification of four and three 287
 historical hurricane events, respectively, that caused heavy 288
 precipitation in the region, as indicated by meteorological data 289
 (<http://pluiesextremes.meteo.fr/>), which allow independent 290
 chronology validation. The sediment deposits triggered by 291
 these events were considered as instantaneous and thus 292
 excluded from the construction of the age model, by removing 293
 the depth interval and associated $^{210}\text{Pb}_{\text{xs}}$ data of each of these 294
 deposits.^{40,42} The logarithmic plot of the event corrected 295
 $^{210}\text{Pb}_{\text{xs}}$ activity shows a general decrease, with two distinct 296
 linear trends (black and dark blue in [Figure 3](#)). According to 297
 the “constant flux, constant sedimentation rate” model⁴⁰ 298
 applied to each segment of the profile, the levels of $^{210}\text{Pb}_{\text{xs}}$ 299
 indicate drastic increases in the sediment accumulation rate 300
 from 3.9 ± 0.6 to 43.3 ± 9.5 $\text{mm}\cdot\text{y}^{-1}$ and from 5.0 ± 0.2 to 301
 22.1 ± 5.1 $\text{mm}\cdot\text{y}^{-1}$ with synchronous changes in 2000 302
 (uncertainty range: 1996–2005) and 1999 (uncertainty: 303
 1995–2004) in the GUA17–01 and GAL17–04 cores, 304
 respectively ([Figure 3](#)). These two age models are well 305
 constrained by the ages of the most intense historical 306
 hurricanes that have hit both islands. This concomitant 307
 increase in sedimentation rates in sediment records located 308
 more than 170 km away from each other might only be 309
 explained by an increase in carbonate productivity in the 310
 marine system or by an increase in terrigenous inputs from the 311
 watersheds. From these age models, the terrigenous mass 312

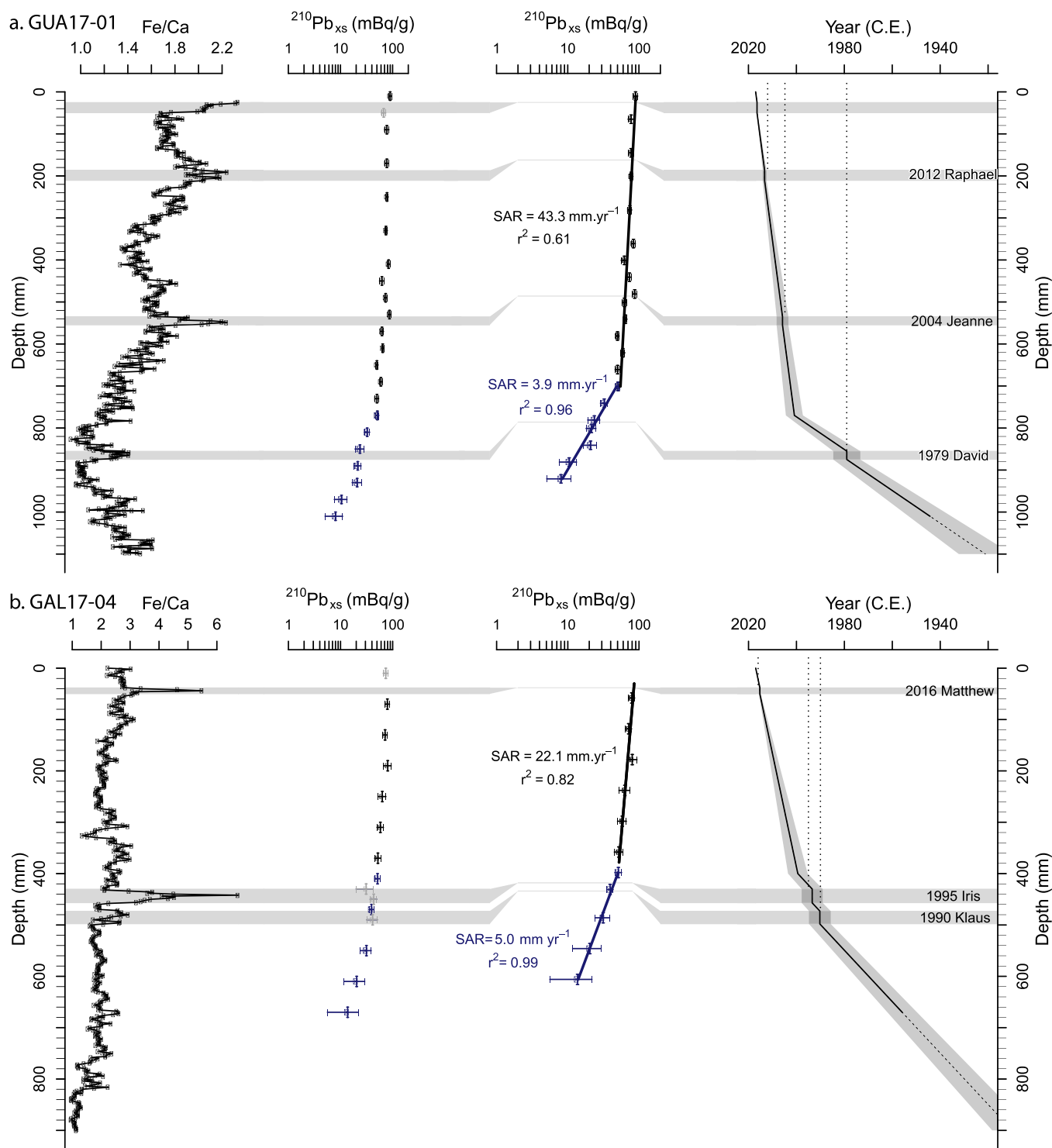


Figure 3. Chronology for the GUA17-01 (a) and GAL17-04 (b) cores with the Fe/Ca, $^{210}\text{Pb}_{\text{xs}}$ activity, instantaneous event-corrected $^{210}\text{Pb}_{\text{xs}}$ activity and age model with uncertainties (gray area) realized with the serac R package.⁴⁰ Dotted lines extending from the black lines indicate age model extrapolation. On the right part of this figure ages and names correspond to historical hurricanes.

313 accumulation was calculated and interpreted as a proxy of soil
 314 erosion in the watershed, indicating that the erosion rate
 315 increased 10- and 4-fold on the basis of the GUA17601 and
 316 GAL17-04 cores, respectively (Figure 4a,b). This interpreta-
 317 tion rules out the hypothesis of an increase in carbonate
 318 precipitation. It is further supported by the observation of a
 319 synchronous increase in the Fe/Ca ratio for GUA core (Figure
 320 4a). For the GAL core we observed a short time lag

(corresponding to less than 2 cm) between Fe/Ca and
 321 terrigenous flux increase which could be related to sampling
 322 resolution (2 cm for short-lived radionuclides not in
 323 continuous versus continuous 2 mm for XRF data) or to the
 324 influence of Iris hurricane (Figure 4b).
 325

Pesticide temporal variations are presented in relation to age
 326 and displayed both in concentrations (Figure S4) and fluxes
 327 (Figure 4). CLD and CLO (a CLD degradation product) 328

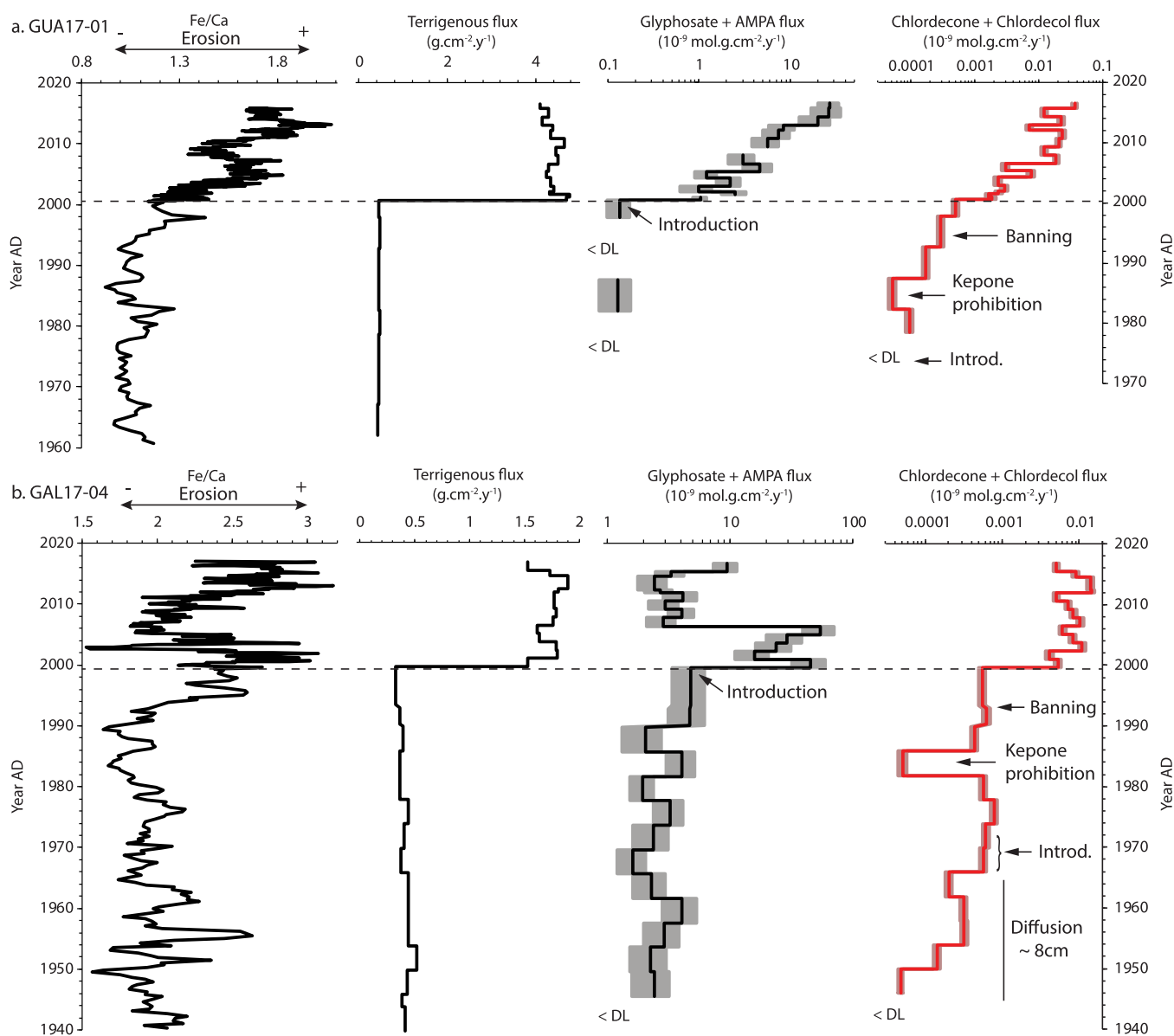


Figure 4. Soil erosion proxies and pesticide flux chronology for Guadeloupe (a) and Martinique (b): Erosion proxies with Fe/Ca and terrigenous fluxes compared to a pesticide chronology (logarithmic scale) reconstructed from the sum of glyphosate and AMPA (glyphosate degradation product) fluxes and the sum of CLD and CLO (one of the CLD degradation products) fluxes. The horizontal dotted line corresponds to the large increase in the sedimentation rate identified in response to a large erosion increase synchronous with glyphosate introduction and CLD flux increases. <DL indicates below the detection limit.

concentrations present similar profiles in both cores (Figure S4) and were thus summed and expressed as fluxes (Figure 4) to account for the large increases in sedimentation rates. In GUA17-01, the CLD + CLO flux is first detected in 1978 \pm 7 yr., just after the introduction of CLD in 1972 and subsequently decreases, which could correspond to the period (1978–1982) between the prohibition of Kepone in the US and the approval of the license for the use of CLD in Curlone by the French authorities in late 1981. Then, the CLD + CLO flux increases, which continues even after its ban in 1993. In 2000 \pm 5 yr., we observed a twofold and more than fivefold increase in the CLD + CLO concentration and flux, respectively. In GAL17-04, CLD and CLO are first observed in very low concentrations at 8 cm (1940–1955), before its introduction dated here at 1970 \pm 6 yr. (Figure S4). This apparent preintroduction record of this compound may be

explained by its possible downward diffusion in sediment, as observed for other chlorinated molecules such as DDT,⁶ or by bioturbation in these shallow marine environments. Then, we observe a decrease in CLD + CLO flux during the prohibition period followed by an increase until the final ban. In 1999 \pm 5 yr., we detected a twofold and more than 10-fold increase in the concentration and flux, respectively.

Finally, between the period of maximum CLD use and the recent high flux, we noted more than 200-fold and 20-fold CLD + CLO flux increases in GUA17-01 and GAL17-04, respectively (Figure 4). The CLO/CLD ratio is higher in the oldest part of the two sediment cores than in the most recent sediment (Figure S4) and in present-day soils in Martinique.⁴³ CLO formation probably results from the reduction of the CLD ketone group under anaerobic conditions,⁴⁴ which are encountered some centimeters below the water–sediment

361 interface. This hypothesis is further supported by the increase
362 in CLO/CLD with depth suggesting long-term CLD
363 degradation within the sediment.

364 **CLD Transfer in CZ.** CLD concentrations in soil surface
365 layers of banana plantations range from 500 to more than 2000
366 $\text{ng}\cdot\text{g}^{-1}$ in the Galion watershed¹⁹ and from 30 to more than
367 24,000 $\text{ng}\cdot\text{g}^{-1}$ in the Pérou watershed.²³ This spatial variability
368 in CLD soil pollution is related both to the duration of the
369 banana cropping period and soil characteristics.¹⁰ Soils in
370 which banana was never planted did not contain any CLD.¹⁹
371 Samples collected in 2002 at the mouth of the Galion River
372 contained 50 and $< 10 \text{ ng}\cdot\text{g}^{-1}$ CLD in suspended matter (>0.7
373 μm) and in sediment, respectively,⁴⁵ reflecting CLD dilution
374 relative to soil concentrations. In comparison, the higher CLD
375 concentrations measured in the recent layers of the two
376 studied sediment cores (1 to 2 $\text{ng}\cdot\text{g}^{-1}$) were still lower than the
377 concentrations in river samples. These differences could be
378 explained both by terrestrial particle dilution by other sediment
379 sources such as uncontaminated fields, channel banks (Figure 2),
380 and marine sediments and by particle size fractionation
381 resulting in coarser sediment fractions in cores (Figure S2)
382 and finer fractions in suspended matter (higher specific surface
383 area) collected in rivers and nearby river mouths.⁴⁶

384 The collection of water samples during two low-intensity
385 floods in December 2013 in the Galion watershed permitted to
386 assess the accumulated mass of transferred CLD in the
387 dissolved and particulate fractions (Figure S5a,b). The CLD
388 content in the particle-bound fraction ranged from 311 to 1059
389 $\text{ng}\cdot\text{g}^{-1}$ (Figure S5c,d). During both floods, the mass of CLD
390 transferred by particles was higher than that transferred in
391 dissolved form (Figure S5), indicating that soil erosion was an
392 important pathway for CLD transfer. In the case of very large
393 floods, such as during storms or cyclonic events, this process
394 could transport huge amounts of CLD from land to sea and the
395 sediment. These results can be related to the erosion occurring
396 in this watershed, identified by short-lived radionuclide
397 measurements in watershed samples (Figure 2). We hence
398 infer that erosion of contaminated soil particles is a major CLD
399 mass transfer process²⁴ which should therefore not be
400 neglected or considered minor, contrary to recent sugges-
401 tions.²²

402 **CZ Erosion Induced by Glyphosate.** The large CLD +
403 CLO flux increases observed around 1999/2000 in both cores
404 are synchronous with a drastic rise in erosion fluxes (Figure 4)
405 and thus probably have a common watershed origin. As the
406 erosion increases synchronously in both sites located on two
407 different islands we can discard local phenomena such as road
408 construction or urban development. Thus, three main
409 hypotheses could explain this observation: (1) climate driver
410 with an increase in precipitation, (2) change in mechanical
411 practice on cropland with extensive tillage, or (3) the extensive
412 use of glyphosate leading to unprotected soil more sensitive to
413 precipitation-induced erosion. First we can discard the climate
414 forcing as no significant precipitation change can be identified
415 from instrumental data during this period in this Caribbean
416 area.⁴⁷ As these two watersheds have similar land use (Figure
417 1d,e) and erosion characteristics of banana and sugar cane
418 fields (Figure 2), we can hypothesize that a concomitant
419 change in agricultural practices caused this erosional increase.
420 Since the early 1970s on banana plantations, the fields were
421 prepared for planting with heavy equipment to enable the
422 planting of banana trees and the drainage of water via ditches
423 dug throughout the fields.⁴⁸ These practices are known to

contribute to soil erosion but cannot explain its large increase
more than 25 yrs. later.

425
426 When these fluxes increase in the two cores, glyphosate and
427 AMPA (glyphosate degradation product) are detected in the
428 GUA17–01 sediment for the first time, and both the
429 concentrations and flux considerably increase in the
430 GAL17–04 sediment (Figure S4). Glyphosate use began in
431 1974, but few banana farmers (only large banana farms)
432 probably used it from the early 1980s until 1997. In 1997, the
433 glyphosate price (Roundup) dropped, causing 90% of farmers
434 to use it from that year onward. Glyphosate is still widely used
435 in the FWI.²⁸ This is in good agreement with the emergence of
436 this chemical in 1999/2000 ± 5 yr. in the two sediment
437 chronologies (Figure 4). In the GAL17–04 core, the
438 glyphosate and AMPA records start earlier (1950). Even if
439 its use in some large farms in the Galion watershed is not
440 totally excluded, as the absence of such large farms in the
441 Pérou watershed points to the diffusion of AMPA as the most
442 probable explanations of downcore migrations of these
443 chemicals⁶ and diffusion and/or bioturbation processes.
444 Since its earliest appearance in GUA17–01, the glyphosate
445 +AMPA flux continuously increased, while in GAL17–04, after
446 a drastic increase, this flux decreased in 2006.5 ± 2.5 yr.
447 before reincreasing in the uppermost layer (Figure 4). This
448 time corresponds to the entry into force of the French law on
449 water (2006–1772), which establishes an untreated area as a
450 buffer around a watercourse, including ditches. In Martinique,
451 important surface drainage networks are present in banana
452 fields. Stopping glyphosate treatment would decrease the
453 export of this chemical through the concentrated flows in these
454 ditches. However, glyphosate is still used in these fields,
455 thereby probably maintaining the transfer of soil particles
456 contaminated by CLD. The difference between our study sites
457 could be linked to the fact that the large farms in the Galion
458 watershed, which are monitored for good practices, quickly
459 adhered to the French law on water.

460 Even if the two watersheds are different in term of farm size,
461 other important watershed characteristics are the same: soil
462 cover, types of cultures, and climate. At both sites, we observed
463 a synchronous increase in CLD + CLO and erosional fluxes
464 when glyphosate was first widely applied to banana fields at the
465 end of the 1990s. The application of glyphosate, which disrupts
466 grass development, has a strong effect on soil erosion as
467 previous demonstrated thought monitoring plots, simulation
468 experiments, and retrospective observation.^{6,25–27,49} Other
469 herbicides, such as paraquat, authorized in the FWI between
470 2003 and 2007, could have caused the same issues. Paraquat
471 was reported to be used along with glyphosate because of
472 glyphosate resistant plants⁵⁰ and intensively used in banana
473 plantations in Latin America.⁵¹ While glyphosate is a systemic
474 herbicide, paraquat, and other herbicides used in the early
475 2000s on banana plantations²⁸ are either selective or
476 nonsystemic. As a result, they do not eliminate all plants on
477 a field, allowing them to recover. Paraquat, for instance is a
478 nonselective but nonsystemic herbicides. It “burns” the leaves
479 of plants while allowing plants to recover from stems or roots.
480 Glyphosate acts differently by killing the whole plants which
481 leaves the soil bare and less maintained by roots leading to
482 potentially enhanced erosion rates. Erosion on bare soil might
483 furthermore be amplified by banana canopies, which exhibit
484 high funneling ratios, favoring runoff even on soils with a high
485 infiltration rate such as Andosols, by localized rainfall
486 redistribution and soil detachment by concentrated flows.⁵²

487 Putting all our observations together, we argue that the
 488 widespread use of a nonspecific systemic herbicide (glypho-
 489 osate) since the late 1990s' could be responsible of an
 490 unprecedented rise in soil erosion and downstream of a major
 491 release of remnant CLD pesticides that were trapped in banana
 492 field soils since their ban in the late 1990s' (Figure 4). As such,
 493 we highlight that new agricultural practices may induce
 494 complex interactions in the CZ dynamic converting soils
 495 from sinks to sources of formerly used pesticides. This
 496 happened in FWI where CLD was probably resurrected by
 497 glyphosate-induced soil erosion (Figure 5) just as in a French

events in the Galion watershed; selected flood samples; 532
²¹⁰Pb_{xs} data for core GUA17-01; ²¹⁰Pb_{xs} data for core 533
 GUA17-04; detailed pesticide analysis protocols (PDF) 534

AUTHOR INFORMATION

Corresponding Author

Pierre Sabatier – Univ. Grenoble Alpes, Univ. Savoie Mont 537
 Blanc, CNRS, EDYTEM, LE Bourget du lac 73376, France; 538
 ● orcid.org/0000-0002-9620-1514; 539
 Email: pierre.sabatier@univ-smb.fr 540

Authors

Charles Mottes – Cirad, UPR HortSys, Le Lamentin, 541
 Martinique F-97285, France; HortSys, Geco, Univ 542
 Montpellier, CIRAD, Montpellier 34398, France 543
 Nathalie Cottin – Univ. Savoie Mont-Blanc, LCME, Le 544
 Bourget du Lac 73376, France 545
 Olivier Evrard – Univ. Paris-Saclay, UVSQ, CEA, CNRS, 546
 LSCE/IPSL, Gif-sur-Yvette F-91191, France 547
 Irina Comte – HortSys, Geco, Univ Montpellier, CIRAD, 548
 Montpellier 34398, France; Cirad, UPR GECO, Capesterre- 549
 Belle-Eau, Guadeloupe F-97130, France 550
 Christine Piot – Univ. Savoie Mont-Blanc, LCME, Le Bourget 551
 du Lac 73376, France 552
 Bastien Gay – Univ. Grenoble Alpes, Univ. Savoie Mont Blanc, 553
 CNRS, EDYTEM, LE Bourget du lac 73376, France; Univ. 554
 Savoie Mont-Blanc, LCME, Le Bourget du Lac 73376, 555
 France 556
 Fabien Arnaud – Univ. Grenoble Alpes, Univ. Savoie Mont 557
 Blanc, CNRS, EDYTEM, LE Bourget du lac 73376, France 558
 Irène Lefevre – Univ. Paris-Saclay, UVSQ, CEA, CNRS, 559
 LSCE/IPSL, Gif-sur-Yvette F-91191, France 560
 Anne-Lise Develle – Univ. Grenoble Alpes, Univ. Savoie Mont 561
 Blanc, CNRS, EDYTEM, LE Bourget du lac 73376, France 562
 Landry Defontaine – Cirad, UPR HortSys, Le Lamentin, 563
 Martinique F-97285, France; HortSys, Geco, Univ 564
 Montpellier, CIRAD, Montpellier 34398, France 565
 Joanne Plet – Cirad, UPR HortSys, Le Lamentin, Martinique 566
 F-97285, France; HortSys, Geco, Univ Montpellier, CIRAD, 567
 Montpellier 34398, France 568
 Magalie Lesueur-Jannoyer – Cirad, UPR HortSys, Le 569
 Lamentin, Martinique F-97285, France; HortSys, Geco, Univ 570
 Montpellier, CIRAD, Montpellier 34398, France 571
 Jérôme Poulenard – Univ. Grenoble Alpes, Univ. Savoie Mont 572
 Blanc, CNRS, EDYTEM, LE Bourget du lac 73376, France 573

Complete contact information is available at: 574
<https://pubs.acs.org/10.1021/acs.est.0c05207> 575

Author Contributions

P.S., C.M., I.C., J.P., and O.E. conceived and designed the 576
 study. Fieldwork sampling was performed by C.M., I.C., J.P., 577
 O.E., and L.D. for soil sampling, P.S. and F.A. for coring, and 578
 J.P., M.L.J., and C.M. for water collection. P.S., N.C., C.P., 581
 B.G., O.E., I.L., and A.L.D. performed the analyses. P.S. wrote 582
 the first draft of the manuscript, with subsequent contribution 583
 by all the authors. 584

Funding

This project EFFLUANT (EFFet à Long terme de l'Utilisation 585
 des pesticides aux ANtilles françaises: pollution et érosion) was 586
 cofunded by the EC2CO/BIOHEFECT structural action of 587
 INSU/CNRS and the Labex DRIIHM, French programme 588
 589

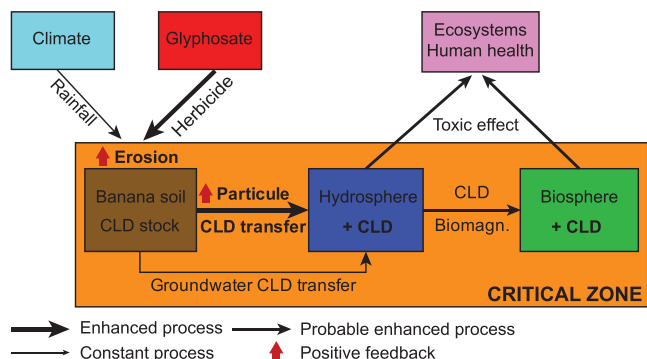


Figure 5. CZ dynamics and responses in FWI relation to past (CLD) and modern (Glyphosate) agricultural practices.

498 vineyard where DDT was resurrected by the same herbicide.⁶
 499 The eroded CLD-contaminated material was transported to
 500 the marine environment bound onto fine particles, where it
 501 became a source of contamination for marine organisms^{13,14,46}
 502 and a potential hazard to human health through seafood
 503 consumption (Figure 5). This mechanism of old pesticide
 504 resurrection by glyphosate is now observed in banana
 505 plantation and vineyard, and perhaps in no tillage agro systems
 506 glyphosate-induced soil erosion could be lower. We recom-
 507 mend future works to answer this hypothesis. The retro-
 508 spective observation applied here allowed us to reconstruct
 509 long-term CZ trajectories under human effort, hence proving
 510 its strength in providing novel and complementary information
 511 to modern-day CZ observatories.³¹

512 Future studies of the environmental fate of pesticides in CZ
 513 should take into account these potential pesticide–environ-
 514 ment interactions from a long-term perspective. In terms of
 515 management options, reducing soil erosion on cropland by
 516 limiting herbicide treatments would lead to the growth of
 517 understory vegetation and ultimately result in the slower
 518 leaching of the pesticides stored in soils. As glyphosate is used
 519 worldwide, it appears crucial that ecotoxicological risk
 520 assessments take into account such mechanisms of remnant
 521 pesticide mobility in the environment through herbicide-
 522 induced erosion.

ASSOCIATED CONTENT

Supporting Information

525 The Supporting Information is available free of charge at
 526 <https://pubs.acs.org/doi/10.1021/acs.est.0c05207>.

527 Land use and sample in the investigated watersheds;
 528 sedimentological and geochemical data in both cores;
 529 biplot of the PCA of XRF geochemical data in both
 530 cores; pesticide chronology expressed in concentration
 531 in both cores; gauging station data during two flood

590 "Investissements d'Avenir" (ANR-11-LABX-0010), which is
591 managed by the ANR, and the OHM Littoral Caraïbe.

592 Notes

593 The authors declare no competing financial interest.

594 ■ ACKNOWLEDGMENTS

595 We thank the French Water Office of Martinique for their
596 financial support of the flood sampling, as well as the farmers
597 of the two watersheds who gave us access to their fields for soil
598 sampling. The authors thank the Laboratoire Souterrain de
599 Modane (LSM) facilities for the gamma spectrometry
600 measurements and Environnement, Dynamique et Territoires
601 de Montagne for the XRF analyses. The authors wish to thank
602 the editor Jennifer A. Field and the three anonymous reviewers
603 who provided comments which greatly improved the original
604 manuscript.

605 ■ ABBREVIATIONS

606 CLD	Chlordecone
607 CLO	Chlordecol
608 AMPA	Aminomethylphosphonic acid
609 DDT	Dichlorodiphenyltrichloroethane
610 FWI	French west indies
611 CZ	Critical zone
612 LOI	Loss of ignition
613 XRF	X-ray fluorescence
614 DBD	Dry bulk density
615 NCIR	Noncarbonate igneous residue
616 CFCS	Constant flux, constant sedimentation rate
618 PCA	Principal component analysis

619 ■ REFERENCES

- 620 (1) Banwart, S. A.; Chorover, J.; Gaillardet, J.; Sparks, D.; White, T.;
621 Anderson, S.; Aufdenkampe, A.; Bernasconi, S.; Brantley, S.;
622 Chadwick, O.; Duffy, C.; Goldhaber, M.; Lehnert, K.; Nikolaidis,
623 N.; Ragnarsdottir, K. *Sustaining Earth's Critical Zone Basic Science and*
624 *Interdisciplinary Solutions for Global Challenges*; 2013; W.L.E., D..
625 (2) Brantley, S. L.; Goldhaber, M. B.; Ragnarsdottir, K. V. Crossing
626 Disciplines and Scales to Understand the Critical Zone. *Elements*
627 **2007**, *3*, 307–314.
628 (3) Syvitski, J. P. M. Impact of Humans on the Flux of Terrestrial
629 Sediment to the Global Coastal Ocean. *Science* **2005**, *308*, 376–380.
630 (4) Steffen, W.; Richardson, K.; Rockstrom, J.; Cornell, S. E.; Fetzer,
631 I.; Bennett, E. M.; Biggs, R.; Carpenter, S. R.; de Vries, W.; de Wit, C.
632 A.; Folke, C.; Gerten, D.; Heinke, J.; Mace, G. M.; Persson, L. M.;
633 Ramanathan, V.; Reyers, B.; Sorlin, S. Planetary Boundaries: Guiding
634 Human Development on a Changing Planet. *Science* **2015**, *347*,
635 1259855–1259855.
636 (5) Borrelli, P.; Robinson, D. A.; Fleischer, L. R.; Lugato, E.;
637 Ballabio, C.; Alewell, C.; Meusburger, K.; Modugno, S.; Schütt, B.;
638 Ferro, V.; Bagarello, V.; Oost, K. V.; Montanarella, L.; Panagos, P. An
639 Assessment of the Global Impact of 21st Century Land Use Change
640 on Soil Erosion. *Nat. Commun.* **2017**, *8*, 2013.
641 (6) Sabatier, P.; Poulencard, J.; Fanget, B.; Reyss, J.-L.; Develle, A.-L.;
642 Wilhelm, B.; Ployon, E.; Pignol, C.; Naffrechoux, E.; Dorioz, J.-M.;
643 Montuelle, B.; Arnaud, F. Long-Term Relationships among Pesticide
644 Applications, Mobility, and Soil Erosion in a Vineyard Watershed.
645 *Proc. Natl. Acad. Sci.* **2014**, *111*, 15647–15652.
646 (7) Gianessi, L. P. The Increasing Importance of Herbicides in
647 Worldwide Crop Production: The Increasing Importance of
648 Herbicides. *Pest Manag. Sci.* **2013**, *69*, 1099–1105.
649 (8) Huggett, R. J.; Bender, M. E. Kepone in the James River. *Environ.*
650 *Sci. Technol.* **1980**, *14*, 918–923.
651 (9) Luellen, D. R.; Vadas, G. G.; Unger, M. A. Kepone in James
652 River Fish: 1976–2002. *Sci. Total Environ.* **2006**, *358*, 286–297.

- (10) Cabidoche, Y.-M.; Achard, R.; Cattán, P.; Clermont-Dauphin, 653
C.; Massat, F.; Sansoulet, J. Long-Term Pollution by Chlordecone of 654
Tropical Volcanic Soils in the French West Indies: A Simple Leaching 655
Model Accounts for Current Residue. *Environ. Pollut.* **2009**, *157*, 656
1697–1705. 657
(11) Clostre, F.; Letourmy, P.; Lesueur-Jannoyer, M. Organo- 658
chlorine (Chlordecone) Uptake by Root Vegetables. *Chemosphere* 659
2015, *118*, 96–102. 660
(12) Coat, S.; Monti, D.; Legendre, P.; Bouchon, C.; Massat, F.; 661
Lepoint, G. Organochlorine Pollution in Tropical Rivers (Guade- 662
loupe): Role of Ecological Factors in Food Web Bioaccumulation. 663
Environ. Pollut. **2011**, *159*, 1692–1701. 664
(13) Dromard, C. R.; Guéné, M.; Bouchon-Navaro, Y.; Lemoine, S.; 665
Cordonnier, S.; Bouchon, C. Contamination of Marine Fauna by 666
Chlordecone in Guadeloupe: Evidence of a Seaward Decreasing 667
Gradient. *Environ. Sci. Pollut. Res.* **2018**, *25*, 14294–14301. 668
(14) Méndez-Fernandez, P.; Kiszka, J. J.; Heithaus, M. R.; Beal, A.; 669
Vandersarren, G.; Caurant, F.; Spitz, J.; Taniguchi, S.; Montone, R. C. 670
From Banana Fields to the Deep Blue: Assessment of Chlordecone 671
Contamination of Oceanic Cetaceans in the Eastern Caribbean. 672
Marine Pollut. Bull. **2018**, *137*, 56–60. 673
(15) Multigner, L.; Kadhel, P.; Rouget, F.; Blanchet, P.; Cordier, S. 674
Chlordecone Exposure and Adverse Effects in French West Indies 675
Populations. *Environ. Sci. Pollut. Res.* **2016**, *23*, 3–8. 676
(16) Multigner, L.; Ndong, J. R.; Giusti, A.; Romana, M.; Delacroix- 677
Maillard, H.; Cordier, S.; Jégou, B.; Thome, J. P.; Blanchet, P. 678
Chlordecone Exposure and Risk of Prostate Cancer. *J. Clin. Oncol.* 679
2010, *28*, 3457–3462. 680
(17) Taitt, H. E. Global Trends and Prostate Cancer: A Review of 681
Incidence, Detection, and Mortality as Influenced by Race, Ethnicity, 682
and Geographic Location. *Am. J. Men's Health* **2018**, *12*, 1807–1823. 683
(18) Clostre, F.; Lesueur-Jannoyer, M.; Achard, R.; Letourmy, P.; 684
Cabidoche, Y.-M.; Cattán, P. Decision Support Tool for Soil Sampling 685
of Heterogeneous Pesticide (Chlordecone) Pollution. *Environ. Sci.* 686
Pollut. Res. **2014**, *21*, 1980–1992. 687
(19) Della Rossa, P.; Jannoyer, M.; Mottes, C.; Plet, J.; Bazizi, A.; 688
Arnaud, L.; Jestin, A.; Woignier, T.; Gaude, J.-M.; Cattán, P. Linking 689
Current River Pollution to Historical Pesticide Use: Insights for 690
Territorial Management? *Sci. Total Environ.* **2017**, *574*, 1232–1242. 691
(20) Woignier, T.; Clostre, F.; Macarie, H.; Jannoyer, M. 692
Chlordecone Retention in the Fractal Structure of Volcanic Clay. *J.* 693
Hazard. Mater. **2012**, *241–242*, 224–230. 694
(21) Fernández-Bayo, J. D.; Saison, C.; Voltz, M.; Disko, U.; 695
Hofmann, D.; Berns, A. E. Chlordecone Fate and Mineralisation in a 696
Tropical Soil (Andosol) Microcosm under Aerobic Conditions. *Sci.* 697
Total Environ. **2013**, *463–464*, 395–403. 698
(22) Cattán, P.; Charlier, J.-B.; Clostre, F.; Letourmy, P.; Arnaud, L.; 699
Gresser, J.; Jannoyer, M. A Conceptual Model of Organochlorine Fate 700
from a Combined Analysis of Spatial and Mid- to Long-Term Trends 701
of Surface and Ground Water Contamination in Tropical Areas 702
(FWI). *Hydrol. Earth Syst. Sci.* **2019**, *23*, 691–709. 703
(23) Crabit, A.; Cattán, P.; Colin, F.; Voltz, M. Soil and River 704
Contamination Patterns of Chlordecone in a Tropical Volcanic 705
Catchment in the French West Indies (Guadeloupe). *Environ. Pollut.* 706
2016, *212*, 615–626. 707
(24) Mottes, C.; Charlier, J.-B.; Rocle, N.; Gresser, J.; Lesueur- 708
Jannoyer, M.; Cattán, P. From Fields to Rivers Chlordecone Transfer 709
in Water. In *Crisis management of chronic pollution: contaminated soil* 710
and human health; Boca Raton: CRC Press, 2016; 121–130. 711
(25) Blavet, D.; De Noni, G.; Le Bissonnais, Y.; Leonard, M.; Maillou, 712
L.; Laurent, J. Y.; Asseline, J.; Lepun, J. C.; Arshad, M. A.; Roose, E. 713
Effect of Land Use and Management on the Early Stages of Soil Water 714
Erosion in French Mediterranean Vineyards. *Soil Tillage Res.* **2009**, 715
106, 124–136. 716
(26) Keesstra, S. D.; Rodrigo-Comino, J.; Novara, A.; Giménez- 717
Morera, A.; Pulido, M.; Di Prima, S.; Cerda, A. Straw Mulch as a 718
Sustainable Solution to Decrease Runoff and Erosion in Glyphosate- 719
Treated Clementine Plantations in Eastern Spain. An Assessment 720
Using Rainfall Simulation Experiments. *CATENA* **2019**, *174*, 95–103. 721

- 722 (27) Liu, H.; Blagodatsky, S.; Giese, M.; Liu, F.; Xu, J.; Cadisch, G.
723 Impact of Herbicide Application on Soil Erosion and Induced Carbon
724 Loss in a Rubber Plantation of Southwest China. *CATENA* **2016**, *145*,
725 180–192.
- 726 (28) Mottes, C.; Lesueur Jannoyer, M.; Le Bail, M.; Guéné, M.;
727 Carles, C.; Malézieux, E. Relationships between Past and Present
728 Pesticide Applications and Pollution at a Watershed Outlet: The Case
729 of a Horticultural Catchment in Martinique, French West Indies.
730 *Chemosphere* **2017**, *184*, 762–773.
- 731 (29) Auer, M. T.; Johnson, N. A.; Penn, M. R.; Effler, S. W.
732 Pollutant Sources, Depositional Environment, and the Surficial
733 Sediments of Onondaga Lake, New York. *J. Environ. Qual.* **1996**,
734 *25*, 46–55.
- 735 (30) Barra, R.; Cisternas, M.; Urrutia, R.; Pozo, K.; Pacheco, P.;
736 Parra, O.; Focardi, S. First Report on Chlorinated Pesticide
737 Deposition in a Sediment Core from a Small Lake in Central Chile.
738 *Chemosphere* **2001**, *45*, 749–757.
- 739 (31) Gaillardet, J.; Braud, I.; Hankard, F.; Anquetin, S.; Bour, O.;
740 Dorfliger, N.; de Dreuzy, J. R.; Galle, S.; Galy, C.; Gogo, S.; Gourcy,
741 L.; Habets, F.; Laggoun, F.; Longuevergne, L.; Le Borgne, T.; Naaim-
742 Bouvet, F.; Nord, G.; Simonneau, V.; Six, D.; Tallec, T.; Valentin, C.;
743 Abril, G.; Allemand, P.; Arènes, A.; Arfib, B.; Arnaud, L.; Arnaud, N.;
744 Arnaud, P.; Audry, S.; Comte, V. B.; Batiot, C.; Battais, A.; Bellot, H.;
745 Bernard, E.; Bertrand, C.; Bessière, H.; Binet, S.; Bodin, J.; Bodin, X.;
746 Boithias, L.; Bouchez, J.; Boudevillain, B.; Moussa, I. B.; Branger, F.;
747 Braun, J. J.; Brunet, P.; Caceres, B.; Calmels, D.; Cappelaere, B.;
748 Celle-Jeanton, H.; Chabaux, F.; Chalikakis, K.; Champollion, C.;
749 Copard, Y.; Cotel, C.; Davy, P.; Deline, P.; Delrieu, G.; Demarty, J.;
750 Dessert, C.; Dumont, M.; Emblanch, C.; Ezzahar, J.; Estèves, M.;
751 Favier, V.; Faucheux, M.; Filizola, N.; Flammarion, P.; Floury, P.;
752 Fovet, O.; Fournier, M.; Francez, A. J.; Gandois, L.; Gascuel, C.;
753 Gayet, E.; Genthon, C.; Gérard, M. F.; Gilbert, D.; Gouttevin, I.;
754 Grippa, M.; Gruau, G.; Jardani, A.; Jeanneau, L.; Join, J. L.; Jourde,
755 H.; Karbou, F.; Labat, D.; Lagadeuc, Y.; Lajeunesse, E.; Lastennet, R.;
756 Lavado, W.; Lawin, E.; Lebel, T.; Le Bouteiller, C.; Legout, C.;
757 Lejeune, Y.; Le Meur, E.; Le Moigne, N.; Lions, J.; Lucas, A.; Malet, J.
758 P.; Marais-Sicre, C.; Maréchal, J. C.; Marlin, C.; Martin, P.; Martins,
759 J.; Martinez, J. M.; Massei, N.; Mauclerc, A.; Mazzilli, N.; Molénat, J.;
760 Moreira-Turcq, P.; Mouglin, G.; Morin, S.; Ngoupayou, J. N.; Panthou,
761 G.; Peugeot, C.; Picard, R.; Pierret, M. C.; Porel, G.; Probst, A.;
762 Probst, J. L.; Rabatel, A.; Raclot, D.; Ravel, L.; Rejiba, F.; René, P.;
763 Ribolzi, O.; Riotte, J.; Rivière, A.; Robain, H.; Ruiz, L.; Sanchez-Perez,
764 J. M.; Santini, W.; Sauvage, S.; Schoeneich, P.; Seidel, J. L.; Sekhar,
765 M.; Sengtaheuanghoung, O.; Silvera, N.; Steinmann, M.; Soruco, A.;
766 Talleg, G.; Thibert, E.; Lao, D. V.; Vincent, C.; Viville, D.; Wagnon,
767 P.; Zitouna, R. OZCAR: The French Network of Critical Zone
768 Observatories. *Vadose Zone J.* **2018**, *17*, No. 180067.
- 769 (32) Desprats, J.F.; Comte, J. P.; Charbier, C. *Cartographie du risque*
770 *de pollution des sols de Martinique par les organochlorés. Rapport Phase*
771 *3. BRGM RP 53262 2004.*
- 772 (33) Tillieut, O. *Cartographie de La Pollution Des Sols de Guadeloupe*
773 *Par La Chlordecone: Rapport Technique 2005–2006. DAF971, SPV*
774 *2006 2005.*
- 775 (34) Rochette, R.; Bonnal, V.; Andrieux, P.; Cattán, P. Analysis of
776 Surface Water Reveals Land Pesticide Contamination: An Application
777 for the Determination of Chlordecone-Polluted Areas in Guadeloupe,
778 French West Indies. *Environ. Sci. Pollut. Res.* **2020**, *27*, 41132–41142.
- 779 (35) Heiri, O.; Lotter, A. F.; Lemcke, G. Loss on Ignition as a
780 Method for Estimating Organic and Carbonate Content in Sediments:
781 Reproducibility and Comparability of Results. *J. Paleolimnol.* **2001**, *25*,
782 101–110.
- 783 (36) Richter, T. O.; van der Gaast, S.; Koster, B.; Vaars, A.; Gieles,
784 R.; de Stigter, H. C.; De Haas, H.; van Weering, T. C. E. The
785 Avaatech XRF Core Scanner: Technical Description and Applications
786 to NE Atlantic Sediments. *Geol. Soc., London, Special Publications*
787 **2006**, *267*, 39–50.
- 788 (37) Le Gall, M.; Evrard, O.; Foucher, A.; Laceby, J. P.; Salvador-
789 Blanes, S.; Manière, L.; Lefèvre, I.; Cerdan, O.; Ayrault, S.
790 Investigating the Temporal Dynamics of Suspended Sediment during
Flood Events with ⁷Be and ²¹⁰Pbxs Measurements in a Drained
Lowland Catchment. *Sci. Rep.* **2017**, *7*, No. 42099.
- (38) Evrard, O.; Chaboche, P.-A.; Ramon, R.; Foucher, A.; Laceby, J.
P. A Global Review of Sediment Source Fingerprinting Research
Incorporating Fallout Radiocesium (¹³⁷Cs). *Geomorphology* **2020**,
362, No. 107103.
- (39) Sabatier, P.; Dezileau, L.; Briquieu, L.; Colin, C.; Siani, G. Clay
Minerals and Geochemistry Record from Northwest Mediterranean
Coastal Lagoon Sequence: Implications for Paleostorm Reconstruc-
tion. *Sediment. Geol.* **2010**, *228*, 205–217.
- (40) Bruel, R.; Sabatier, P. Serac: An R Package for Shortlived
Radionuclide Chronology of Recent Sediment Cores. *J. Environ.*
Radioact. **2020**, *225*, No. 106449.
- (41) Delaval, A.; Duffa, C.; Radakovitch, O. A Review on Cesium
Desorption at the Freshwater-Seawater Interface. *J. Environ. Radioact.*
2020, *218*, No. 106255.
- (42) Arnaud, F.; Lignier, V.; Revel, M.; Desmet, M.; Beck, C.;
Pouchet, M.; Charlet, F.; Trentesaux, A.; Tribouillard, N. Flood and
Earthquake Disturbance of ²¹⁰Pb Geochronology (Lake Anterne,
NW Alps). *Terra Nova* **2002**, *14*, 225–232.
- (43) Chevallier, M. L.; Della-Negra, O.; Chaussonnerie, S.;
Barbançe, A.; Muselet, D.; Lagarde, F.; Darii, E.; Ugarte, E.;
Lescop, E.; Fonknechten, N.; Weissenbach, J.; Woignier, T.;
Gallard, J.-F.; Vuilleumier, S.; Imfeld, G.; Le Paslier, D.; Saaidi, P.-
L. Natural Chlordecone Degradation Revealed by Numerous
Transformation Products Characterized in Key French West Indies
Environmental Compartments. *Environ. Sci. Technol.* **2019**, *53*, 6133–
6143.
- (44) Macarie, H.; Novak, I.; Sastre-Conde, I.; Labrousse, Y.;
Archelas, A.; Dolfing, J. Theoretical Approach to Chlordecone
Biodegradation. In *Crisis management of chronic pollution: contami-
nated soil and human health*; Boca Raton: CRC Press, 2016; 191–209.
- (45) Bocquené, G.; Franco, A. Pesticide Contamination of the
Coastline of Martinique. *Marine Pollut. Bull.* **2005**, *51*, 612–619.
- (46) Bertrand, J. A.; Abarnou, A.; Bodiguel, X.; Guyader, O.; Reynal,
L.; Robert, S. Assessment of Chlordecone Content in the Marine Fish
Fauna around the French West Indies Related to Fishery Manage-
ment Concerns. In *Crisis management of chronic pollution: contami-
nated soil and human health*; Boca Raton: CRC Press, 2016; 105–117.
- (47) Jones, P. D.; Harpham, C.; Harris, I.; Goodess, C. M.; Burton,
A.; Centella-Artola, A.; Taylor, M. A.; Bezanilla-Morlot, A.; Campbell,
J. D.; Stephenson, T. S.; Joslyn, O.; Nicholls, K.; Baur, T. Long-Term
Trends in Precipitation and Temperature across the Caribbean:
PRECIPITATION AND TEMPERATURE TRENDS ACROSS
THE CARIBBEAN. *Int. J. Climatol.* **2016**, *36*, 3314–3333.
- (48) Champion, J. *Les Possibilités de Mécanisation En Culture*
Bananière L. Fruit 1970, 669–683.
- (49) Mickelson, S. K.; Boyd, P.; Baker, J. L.; Ahmed, S. I. Tillage and
Herbicide Incorporation Effects on Residue Cover, Runoff, Erosion,
and Herbicide Loss. *Soil Tillage Res.* **2001**, *60*, 55–66.
- (50) Beckie, H. J. Herbicide-Resistant Weed Management: Focus on
Glyphosate. *Pest Manag. Sci.* **2011**, DOI: 10.1002/ps.2195.
- (51) Henriques, W.; Jeffers, R. D.; Lacher, T. E.; Kendall, R. J.
Agrochemical Use on Banana Plantations in Latin America: A
Perspectives on Ecological Risk. *Environ. Toxicol. Chem.* **1997**, *16*,
91–99.
- (52) Cattán, P.; Bussière, F.; Nouvellon, A. Evidence of Large
Rainfall Partitioning Patterns by Banana and Impact on Surface
Runoff Generation. *Hydrol. Process.* **2007**, *21*, 2196–2205.